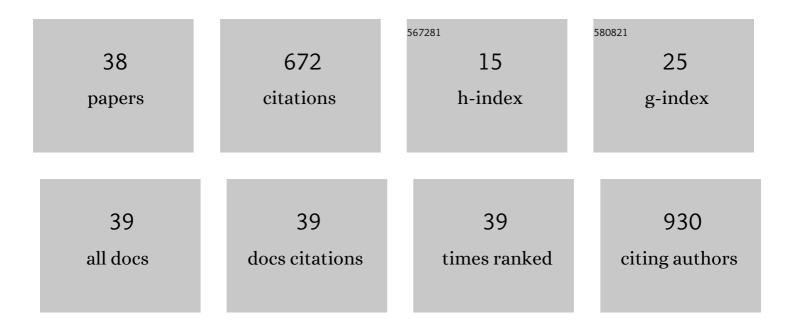
Yanwei Zeng

List of Publications by Year in descending order

Source: https://exaly.com/author-pdf/5664219/publications.pdf Version: 2024-02-01



YANWELZENC

#	Article	IF	CITATIONS
1	Resource utilization of waste V2O5-based deNOx catalysts for hydrogen production from formaldehyde and water via steam reforming. Journal of Hazardous Materials, 2020, 381, 120934.	12.4	34
2	Novel porous ceramic sheet supported metal reactors for continuous-flow catalysis. Catalysis Today, 2020, 358, 324-332.	4.4	13
3	Steam reforming of formaldehyde for generating hydrogen and coproducing carbon nanotubes for enhanced photosynthesis. Catalysis Science and Technology, 2020, 10, 4436-4447.	4.1	6
4	NaCl-induced nickel–cobalt inverse spinel structure for boosting hydrogen evolution from ethyl acetate and water. Journal of Materials Chemistry A, 2019, 7, 1700-1710.	10.3	19
5	Key Role of Lanthanum Oxychloride: Promotional Effects of Lanthanum in NiLaO <i>_y</i> /NaCl for Hydrogen Production from Ethyl Acetate and Water. Small, 2018, 14, e1800927.	10.0	12
6	Preparation of highly (001)-oriented α-Fe2O3 film on Si-substrate from drop coated BaFe12O19 via barium diffusion-induced transformation. Ceramics International, 2017, 43, 5362-5366.	4.8	1
7	Preparation of 2D α-Fe ₂ O ₃ platelets via a hydrothermal heterogeneous growth approach and study of their magnetic properties. New Journal of Chemistry, 2017, 41, 6436-6444.	2.8	4
8	Processing temperature tuned interfacial microstructure and protonic and oxide ionic conductivities of well-sintered Sm0.2Ce0.8O1.9- Na2CO3 nanocomposite electrolytes for intermediate temperature solid oxide fuel cells. Journal of Power Sources, 2017, 360, 114-123.	7.8	14
9	Enhanced photocatalytic properties of CdS -decorated BiPO4 heterogeneous semiconductor catalyst under UV-light irradiation. Journal of Alloys and Compounds, 2017, 729, 189-197.	5.5	27
10	Porous Fe ₃ O ₄ –NCs-in-Carbon Nanofoils as High-Rate and High-Capacity Anode Materials for Lithium-Ion Batteries from Na–Citrate-Mediated Growth of Super-Thin Fe–Ethylene Glycolate Nanosheets. ACS Applied Materials & Interfaces, 2016, 8, 7977-7990.	8.0	30
11	Preparation of SDC–NC nanocomposite electrolytes with elevated densities: influence of prefiring and sintering treatments on their microstructures and electrical conductivities. RSC Advances, 2016, 6, 99615-99624.	3.6	5
12	One-step synthesis of single phase micro-sized BaFe12O19 hexaplates via a modified hydrothermal approach. Materials Chemistry and Physics, 2016, 184, 241-249.	4.0	12
13	An Investigation of Protonic and Oxide Ionic Conductivities at the Interfacial Layers in SDC-LNC Composite Electrolytes. Electrochimica Acta, 2016, 212, 583-593.	5.2	13
14	Temperature- and time-tuned morphological evolution of polyhedral magnetite nanocrystals and their facet-dependent high-rate performance for lithium-ion batteries. Journal of Alloys and Compounds, 2016, 676, 347-355.	5.5	15
15	Magnetic Properties of a Highly Textured Barium Hexa-Ferrite Quasi-Single Crystal and Its Application in Low-Field Biased Circulators. Journal of Electronic Materials, 2016, 45, 5069-5073.	2.2	11
16	Dopant-induced shape evolution of polyhedral magnetite nanocrystals and their morphology/component-dependent high-rate electrochemical performance for lithium-ion batteries. RSC Advances, 2016, 6, 53331-53338.	3.6	2
17	Hierarchically porous Fe ₃ O ₄ /C nanocomposite microspheres via a CO ₂ bubble-templated hydrothermal approach as high-rate and high-capacity anode materials for lithium-ion batteries. Journal of Materials Chemistry A, 2016, 4, 5898-5908.	10.3	71
18	Effects of magnetic pre-alignment of nano-powders on formation of high textured barium hexa-ferrite quasi-single crystals via a magnetic forming and liquid participation sintering route. Journal of Magnetism and Magnetic Materials, 2015, 382, 188-192.	2.3	12

Yanwei Zeng

#	Article	IF	CITATIONS
19	Highly dispersed spherical Bi3.25La0.75Ti3O12 nanocrystals via topotactic crystallization of aggregation-free gel particles from an effective inverse miniemulsion sol–gel approach. Journal of Nanoparticle Research, 2015, 17, 1.	1.9	1
20	Preparation of spherical Bi3.25La0.75Ti3O12 nanocrystals by a sol-gel inverse mini-emulsion approach. Electronic Materials Letters, 2014, 10, 1-4.	2.2	5
21	Synthesis of manganese–zinc ferrite nanopowders prepared by a microwave-assisted auto-combustion method: Influence of sol–gel chemistry on microstructure. Materials Science in Semiconductor Processing, 2014, 23, 50-57.	4.0	13
22	Solvothermal synthesis of La9.33Si6O26 nanocrystals and their enhancing impacts on sintering and oxygen ion conductivity of Sm0.2Ce0.8O1.9/La9.33Si6O26 composite electrolytes. International Journal of Hydrogen Energy, 2014, 39, 6295-6306.	7.1	10
23	Investigation of Sm _{0.2} Ce _{0.8} O _{1.9} /Na ₂ CO ₃ Nanocomposite Electrolytes: Preparation, Interfacial Microstructures, and Ionic Conductivities. ACS Applied Materials &: Interfaces. 2013. 5. 12876-12886.	8.0	34
24	One-step synthesis of yttrium orthoferrite nanocrystals via sol–gel auto-combustion and their structural and magnetic characteristics. Materials Chemistry and Physics, 2013, 137, 877-883.	4.0	43
25	Influence of pH on the property of apatite-type lanthanum silicates prepared by sol-gel process. Journal Wuhan University of Technology, Materials Science Edition, 2012, 27, 841-846.	1.0	6
26	Electrical properties and thermal expansion of cobalt doped apatite-type lanthanum silicates based electrolytes for IT-SOFC. Materials Research Bulletin, 2012, 47, 719-723.	5.2	25
27	Low-temperature synthesis and microstructure-property study of single-phase yttrium iron garnet (YIG) nanocrystals via a rapid chemical coprecipitation. Materials Chemistry and Physics, 2011, 125, 646-651.	4.0	38
28	Preparation and characterization of Ce0.8Sm0.2O1.9(SDC)–carbonates composite electrolyte via molten salt infiltration. Materials Letters, 2011, 65, 2751-2754.	2.6	34
29	Effects of In3+-substitution on the structure and magnetic properties of multi-doped YIG ferrites with low saturation magnetizations. Journal of Magnetism and Magnetic Materials, 2011, 323, 611-615.	2.3	29
30	Synthesis and characterization of Al3+-doped La9.33Ge6O26 intermediate temperature electrolyte for SOFCs. Materials Science and Engineering B: Solid-State Materials for Advanced Technology, 2010, 171, 50-55.	3.5	3
31	Preparation of SmxCe1â^'xO2(SDC) electrolyte film with gradient structure via a gas-phase controlling convection–diffusion approach on porous substrate. Advances in Colloid and Interface Science, 2010, 161, 181-194.	14.7	3
32	Electrochemical redox pattern and allied interactive behaviour of FAD on aÂruthenium-modified glassy carbon electrode surface. Physics and Chemistry of Liquids, 2010, 48, 708-722.	1.2	3
33	Modeling investigation of gradient electrolyte films deposited via convection–diffusion on porous electrode substrates. Journal of Power Sources, 2008, 178, 309-315.	7.8	4
34	Direct synthesis of La9.33Si6O26 ultrafine powder via sol–gel self-combustion method. Journal of Alloys and Compounds, 2008, 458, 378-382.	5.5	35
35	Porosity–permeability and textural heterogeneity of reservoir sandstones from the Lower Cretaceous Putaohua Member Of Yaojia Formation, Weixing Oilfield, Songliao Basin, Northeast China. Marine and Petroleum Geology, 2007, 24, 109-127.	3.3	37
36	Modeling of chloride diffusion in hetero-structured concretes by finite element method. Cement and Concrete Composites, 2007, 29, 559-565.	10.7	38

#	Article	IF	CITATIONS
37	Convection–diffusion derived gradient films on porous substrates and their microstructural characteristics. Journal of Materials Science, 2007, 42, 2387-2392.	3.7	4
38	A modeling investigation on the electrochemical behavior of porous mixed conducting cathodes for solid oxide fuel cells. Journal of Power Sources, 2005, 139, 35-43.	7.8	6